

# Non-ohmic properties of highly resistive dust layers – experimental studies and numerical modelling under OpenFOAM®

U. Riebel<sup>1</sup>, Y. Aleksin<sup>1</sup>, A. L. Vora<sup>1</sup>

<sup>1</sup> Chair of Particle Technology, Brandenburg Technical University, Postf. 101344, 03013 Cottbus, Germany

Corresponding author: [riebel@b-tu.de](mailto:riebel@b-tu.de)

Keywords: ESP, Back Corona, Dust Resistivity, Dust Resistivity Measurement

## 1. Introduction

Back corona and dust resistivity are well known topics in electrostatic precipitation. Back corona results from high dust resistivity and occurs when the field strength in the dust layer surpasses a critical value  $E_{\text{crit}}$ , which is typically found to be in the order of 15 to 30 kV/cm [1-5].

Besides the resistivity  $\rho$ , the current density is the main parameter. According to current understanding, the field  $E$  inside the dust cake is calculated using Ohm's law:  $E = i \varphi < E_{\text{crit}}$  (1). Hence, possible actions against back corona include a reduction of the specific resistivity  $\rho$  by dust conditioning, or a reduction of the current density  $i$ , for example by pulsed corona operation. Much work has been devoted to study the dependence of  $\rho$  on dust composition, temperature, humidity, adsorption layers and dust layer porosity, and a variety of different set-ups for dust resistivity measurements has been proposed. Even though some authors report a dependence of  $\rho$  on current density or field strength [4], dust resistivity is mostly seen as a material property.

In contrast, the literature provides clear hints that the occurrence of the back corona obviously depends on the thickness of the dust layer on the collecting electrode [2, 6, 7]. For thicker dust layers, the back corona is observed much earlier, that is at lower current densities. White [2] states that the critical current density for the onset of back corona is significantly higher for positive corona compared to negative corona. Clearly, all these effects in conflict with the statements of Eq. (1) and with the concept of the "critical field", and they are not compatible with the assumption of ohmic dust resistivity.

Therefore, and for a better understanding of electric conduction through dust layers and of back corona in electrostatic precipitation, the authors have studied the mechanisms of current transport through highly resistive dust layers in detail. The result is, that highly resistive dust layers must be seen as dielectrics or electret media, which will be discussed in the following.

## 2. Basic properties of electret materials

Electrets [8] are dielectric materials which are able to produce external electrostatic fields either due to electric charges which are caught inside the material, or due to electric dipoles which are frozen in a certain orientation. As these materials do not contain any

mobile (conduction band) charge carriers, electric conduction through electrets is generally connected to the injection of negative (electrons) or positive (holes) charge carriers. Inversely, the detection of such charge carriers (or excess charges) gives proof of electret behavior.

The overall concentration of charge carriers in an electret layer is generally limited to a maximum which is derived from Maxwell's first equation and is known as the space charge limit. But, a lower limitation is possible for example due to the kinetics of charge carrier injection.

Injection of charge carriers from an electrode requires an activation energy which is typically in the range from 0.5 to 5 eV, depending on the materials which make the contact to the electret layer which is under investigation. As the work of injection  $\phi_i$  is quite high compared to the thermal energy  $kT$  of the charge carriers ( $kT = 0,026$  eV @ 300 K), the process of charge injection is limited depending on the temperature or on the local field strength. This process is known as "thermionic field emission" or "Schottky emission". Further,  $\phi_i$  generally is different for electrons and holes. In combination with a non-symmetric contact situation at the electret, this produces a polarity-dependent conductivity. Also, a non-symmetric contact situation favors the accumulation of a unipolar excess charge in the electret.

Injected charge carriers move through the electret layer from both sides towards the opposite electrode. When free electrons and holes meet, they disappear by recombination.

Further, both electrons and holes can lose their mobility by trapping. Detrapping, the reverse process, is possible by thermal energy, and the Poole-Frenkel-effect describes how the effective activation energy for detrapping is lowered by strong fields. Trapping is very important. In combination with the space charge limited charge carrier concentration, trapping leads to a strong reduction of mobile charge carriers with time, and to a strong dependence of resistivity on time.

Some important properties of electret layers can be understood from a simple model just considering space charge limited current [9-11]. The model assumes that only mobile unipolar charge carriers exist. Accordingly, the voltage drop  $\Delta U$  across the electret layer is linked to the (average) space charge density  $C_{\text{el}}$  by

$$\Delta U = \frac{1}{2} \times \frac{C_{el}}{\epsilon} \times \Delta s^2 \quad (1)$$

where  $\Delta s$  is the layer thickness. Substituting this into the equation for space charge limited current by Mott and Gurney [9-11]

$$i_{sclc} = 9 \frac{\epsilon Z_{el} (\Delta U)^2}{8 (\Delta s)^3} \quad (2)$$

and combining with the definition of resistivity  $\rho_{el}$

$$\rho_{el} = \frac{E}{i} = \frac{\Delta U}{I} \times \frac{A}{s} \quad (3)$$

( $i$  current density,  $I$  current,  $E$  field strength,  $A$  area) gives the apparent resistivity for space charge limited current as:

$$\rho_{el,sclc} = \sqrt{\frac{8}{9\epsilon Z_{el}}} \frac{\sqrt{\Delta s}}{\sqrt{i_{sclc}}} \quad (4)$$

This result indicates that dust layer resistivity  $\rho_{el}$  should increase with layer thickness and decrease with current density.

### 3. Dust layers in an ESP

For a dust layer in an ESP exposed to a corona discharge, the injection situation is highly nonsymmetric, as the injection energy  $\phi_i$  for charge carriers from a corona discharge appears to be near to zero. As a consequence, dust layers exposed to a corona discharge generally show a strong excess charge with a polarity equal to the polarity of the corona.

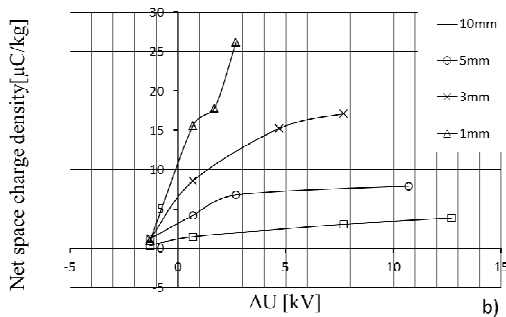


Figure 1. Space charge density measured (Faraday cup method) on layers of Acrylat powders after exposition to positive corona.  $\Delta U$  is the difference to corona onset voltage

As an example, we show the charge density measured on layers of Acrylat (a polymer powder) with different layer thicknesses after exposition to corona discharges with different voltages.

### 4. Measurements of dust resistivity

For the measurement of dust resistivity, mainly two types of arrangement are used: In the corona-sample-electrode (CSE) arrangement (Fig. 2a) the dust layer is in contact with an electrode on one side, while the other side is exposed to the corona discharge. This gives a pretty good imitation of the situation of the dust in a real ESP. Nevertheless, probably most of the measurements are made with an electrode-sample-electrode (ESE) arrangement (Fig. 2b), as handling and evaluation are more simple.

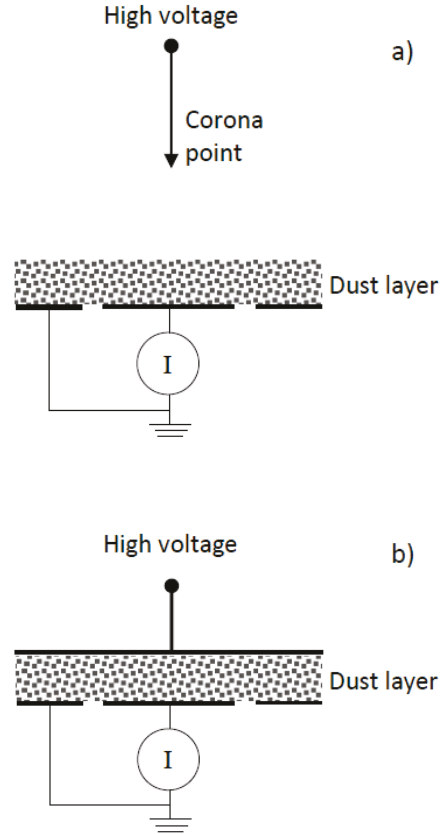


Figure 2. Configurations for the measurement of dust resistivity: Corona-Sample-Electrode (CSE) above, Electrode-Sample-Electrode (ESE) below

A general problem with all measurements of dust resistivity are the time effects originating mainly from the immobilization of charges inside the highly resistive material. Not surprising, these time effects are especially pronounced in the range of higher resistivities. Additional time effects may originate from chemical reactions in gas discharges, namely the formation of  $\text{NO}_x$  which is adsorbed to the surfaces and can lead to a decrease of resistivity when several measurements are made on the same sample consecutively.

An example of time effects is given in Fig. 3, showing the current density measured on samples of Acrylat with different combinations of voltage difference and layer thickness. Obviously, resistivity chan-

ges by several orders of magnitude due to charge carrier immobilization, and this process continues well beyond the 2000 s covered by this measurement. It is also evident that the time effect is more pronounced in the case of low field strength. With high field strength, the Poole-Frenkel-Effect [12] reduces the detrapping energy, and the equilibrium between mobile and trapped charge carriers is shifted more towards the mobile ones.

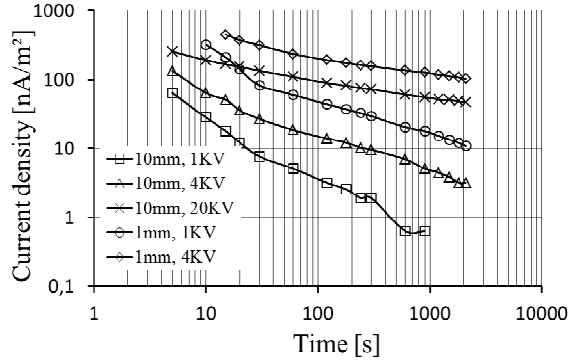


Figure 3. Time dependent current densities measured on samples of Acrylat, various layer thicknesses and voltages, ESE arrangement

Time effects superimpose on all measurements of dust resistivity. Hence, a strict time schedule has to be kept in order to obtain reproducible results. When several measurement points are taken from one sample, for example when varying current density, the sequence of and the time interval between the measurement points has to be considered for a better understanding.

Fig. 4 shows resistivity measurements executed on a Boehmite powder (PURAL NF<sup>®</sup>) using the CSE arrangement. The current density was varied by increasing the voltage applied to the samples step by step. The current readings were taken always 30 s after applying the new voltage. The curves end just before the electrical breakthrough occurs. The initial rise of resistivity with increasing current density and the maximum on the resistivity curves are mainly due to time effects and are not found when the current density is measured with stepwise decreasing voltage. Besides that, we see strong effects from layer thickness and current density.

Fig. 5 shows corresponding measurements taken with the ESE arrangement – all other conditions were identical to the measurements shown in Fig. 4. However, the results obtained with both methods are not at all comparable. The explanation is found in the different conditions of charge injection into the layer. The CSE arrangement is non-symmetric and leads to a high unipolar charging with the polarity of the corona. In contrast, the ESE arrangement is symmetric. In case that the work of injection is comparable for electrons and holes (as it seems to be the case here), there is a symmetric bipolar charging from both electrodes, while the volume-averaged net space charge remains

close to zero. As the potential drops produced by the two oppositely charged sublayers cancel out to a large degree, the resistivities are much lower, and they do not depend so much on the layer thickness.

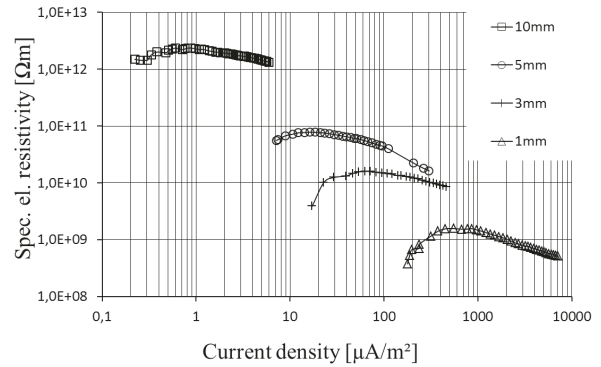


Figure 4. Resistivity measurement (CSE) on PURAL NF<sup>®</sup> for varied current density and different layer thickness

Both ESE and CSE results show pretty good agreement to the theoretical expectation for space charge limited current, according to which  $\rho_{el} \sim (j)^{-0.5}$  is expected.

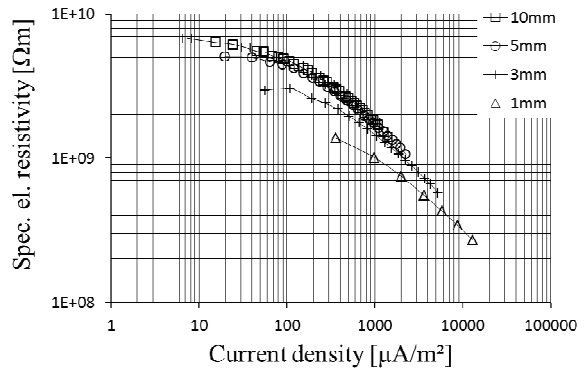


Figure 5. Resistivity measurement on PURAL NF<sup>®</sup>. Conditions corresponding to the measurement shown in Fig. 4, but ESE arrangement

## 5. Simulations

For a numerical simulation of charge transport through highly resistive dust layers, the kinetic equations for injection, deterministic and diffusive motion, trapping, detrapping and recombination of charge carriers were established in analogy to previous approaches [11,13]. Together with Maxwell's 1<sup>st</sup> equation, these equations were introduced into the CFD software package OpenFOAM<sup>®</sup>.

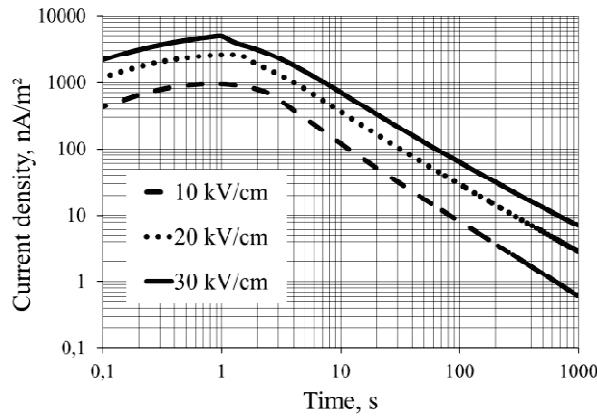


Figure 6. Part of simulation results for 3 mm layer with parameters adapted to measurements for Acrylat, compare Fig. 3

In a first approach, we used a continuum approach, that is, the dust layer including dust particles, gas filled pores and contact points between the particles is modelled a homogeneous material with “effective” parameters describing the charge carrier kinetics [PowTechn.]. More detailed models are under development, but not yet ready for use. In spite of the gross simplifications, the continuum model seems to be able to reproduce complex measurement results in a rather satisfactory way.

Fig. 6 gives simulation results for the time dependent current through layers of Acrylat, whereby the kinetic data were optimized (by trial and error) to obtain a “best fit” to the experimental data shown in Fig. 3. The variation of slope with the field strength results from the Poole-Frenkel-effect.

Fig. 7 shows simulated data for the time dependent field strength inside an Acrylat dust layer of 5 mm thickness during exposure to a given field strength of 10 kV/cm. The simulation result shown uses kinetic data adapted to ESE-measurements on Acrylat - compare Fig. 3 for the original measurement data and Fig. 6 for corresponding simulations of current uptake. It is seen very well how the field strength near the electrodes is reduced, which results from the injection of charge carriers of both polarities into the material, and leads to a strong reduction of charge injection with time. Simultaneously, the field strength in the central part of the layer is increased, which might promote the migration and the detrapping in this part. But it is also seen, that the charge carriers have not yet reached the central part of the layer.

The charging of the dust layers during current transport may also explain the mechanism how craters are formed in a dust layer due to back corona. As the sketch in Fig. 8 shows, the dust directly adjacent to the precipitation electrode is repelled from this electrode and attracted by the corona electrode due to its level of high space charge. The mechanical instability which is created in this way may lead to the formation of the typical craters.

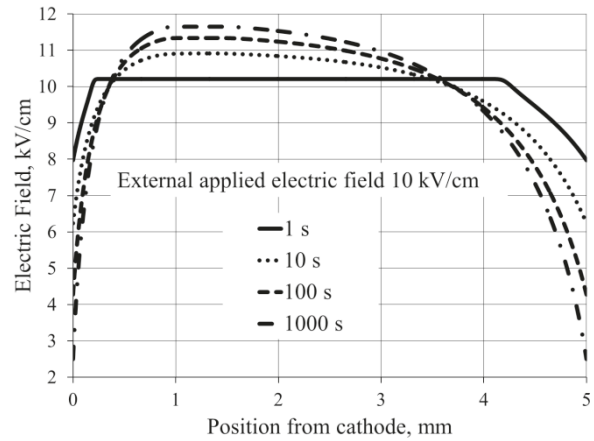


Figure 7. Temporal variation of electric field distribution inside a 5 mm layer of Acrylat, simulation result

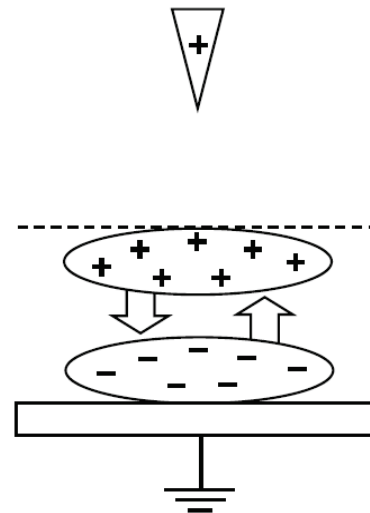


Figure 8. The mechanism of crater formation by dust layer space charge at back corona conditions, example for positive corona. From [11]

## 6. Conclusions

Highly resistive dust layers show strongly non-ohmic properties:

Most strikingly, resistivity may vary by several orders of magnitude with time.

Also, the experimental arrangement can change the resistivity results by orders of magnitude: When resistivity is measured with the dust layer exposed to a corona discharge (imitating the situation in a real ESP),  $\rho_{el}$  depends strongly on the layer thickness. Meanwhile the same dust does not show the strong layer thickness dependence when electrodes are placed on both sides of the dust layer, and also time effects are much less prominent.

The dependence of resistivity on current density agrees well with the theoretical expectation for space charge limited current.

Additional findings include that dusts that have been exposed to resistivity measurements show a high

level of electrostatic charging afterwards. Typically, a bipolar charging of the dust layers occurs.

Crater formation, as it is typical for back corona, can be explained from an instability of the dust layer arising from the bipolar space charge within the layers.

In view of technical applications, the common procedures of dust resistivity measurement have to be reviewed critically. The huge difference between results obtained with corona-sample-electrode arrangements and with electrode-sample-electrode arrangements, resp., shows that the measurement setup has to be adapted closely to the real situation. The same holds true for the effects of measurement time and current density.

Altogether, the results show that the so-called “dust resistivity” is not a material specific property and therefore not suitable to characterize the electrical properties of dust layers sufficiently. Besides the widely discussed influences from the state of the dust layer (depending on temperature, humidity, adsorption layers, particle size distribution, porosity and gas pressure), the resistivity depends significantly and specifically on the experimental arrangement (ESE or CSE), on the layer thickness and on the current density. Significant time effects and memory or hysteresis effects have to be considered in all measurements on highly resistive dusts.

#### Acknowledgements

Most of the theoretical results and some of the experiments were obtained in a research project which is part of DFG-SPP 1486 “PiKo - Particles in Contact” and was funded by DFG grants Rie533/14-1 to /14-3. Most of the experiments on dust layers were executed by Mario Moragalla as part of his master thesis with funding by ESTATIK Foundation Guenter and Sylvia Luettgens, Odenthal, Germany.

#### References

- [1] White H., Industrial Electrostatic Precipitation, Addison-Wesley, Reading MA, 1963
- [2] White H., J. of the Air Pollution Control Association 24 (1974) 314 – 338.
- [3] Masuda S., Chang J.-S., Kelly A.J., Crowley J.M. (eds), Handbook of Electrostatic Processes, Marcel Dekker, Inc., 1995
- [4] Wiggers H., VGB Power Tech 3 (2007) 93 – 96.
- [5] Pieloth D., Wiggers H., Walzel P., Chem. Eng. Technol. 37 (4) (2014) 627-634
- [6] Popa G.N. et al., Acta Technica Corviniensis-Bulletin of Engineering, Romania, 5 (2) (2012) 93-96, ISSN 2067-3809
- [7] Hoferer B., A. J. Schwab, Local occurrence of back corona at the dust layer of electrostatic precipitators. Electrical Insulation and Dielectric Phenomena, Annual Report conference on (Vol. 1), 2000. DOI 10.1109/CEIDP.2000.885235 (10.03.2015)
- [8] Sessler G.M., (ed.), Electrets, 3rd ed., Laplacian Press, California, 1998
- [9] Mott N. F., Gurney R.W., Electronic Processes in Ionic Crystals, Oxford University Press, 1940
- [10] Lampert M.A., Phys. Rev. 103 (1956) 1648
- [11] Aleksin Y., Vora A., Riebel U., Powder Technology 294 (2016) 353–364
- [12] Frenkel J., Phys. Review, 54(8) (1938) 647-648
- [13] Serdyuk Y.V., Gubanski S.M., IEEE Transact. on Dielectrics and Electrical Insulation, 12 (4) (2005), 100-110.